Electronic Supplementary Information for

Green and Facile Synthesis of a Theranostic Nanoprobe with Intrinsic Biosafety and Targeting Ability

Cai Zhang,[b†] Li Zhou,[a†] Jing Zhang,[a] Yan-Yan Fu,[a] Xuejun Zhang,[a] Chunshui Yu,[ab] Shao-Kai Sun,[*a] and Xiu-Ping Yan[c]

a. School of Medical Imaging, Tianjin Medical University, Tianjin 300203, China

b. Department of Radiology, Tianjin Key Laboratory of Functional Imaging, Tianjin Medical University General Hospital, Tianjin 300052, China.

c. College of Chemistry, Research Center for Analytical Sciences, State Key Laboratory of Medicinal Chemical Biology (Nankai University), Tianjin Key Laboratory of Molecular Recognition and Biosensing, and Collaborative Innovation Center of Chemical Science and Engineering (Tianjin), Nankai University, 94 Weijin Road, Tianjin 300071, China.

[*]Corresponding author. E-mail: shaokaisun@163.com

Experimental Section

The assessment of colloidal and structural stability of Tf-ICG nanoparticles. Tf-ICG nanoparticles (1 mg/mL) and ICG (0.14 mg/mL) were dispersed in various media including water, NaCl (w/w, 0.9%), PBS (pH 7.4, 10 mM), fetal calf serum (FBS). Then photos were taken at different time points to monitor the colloidal stability.

The possible dissociation of ICG from the nanoparticles dispersed in various media was also investigated at different incubation time (1-14 d) via ultrafiltration centrifugation. The contents of ICG in filtrates were determined based on absorption spectra.

The structural stability of Tf-ICG nanoparticles in the presence of BSA was investigated. Tf-ICG nanoparticles were added into a dialysis bag and dialyzed against BSA solution. It should note that the content of Tf and BSA was same. The content of ICG left in Tf-ICG nanoparticles was determined via absorption spectrum.

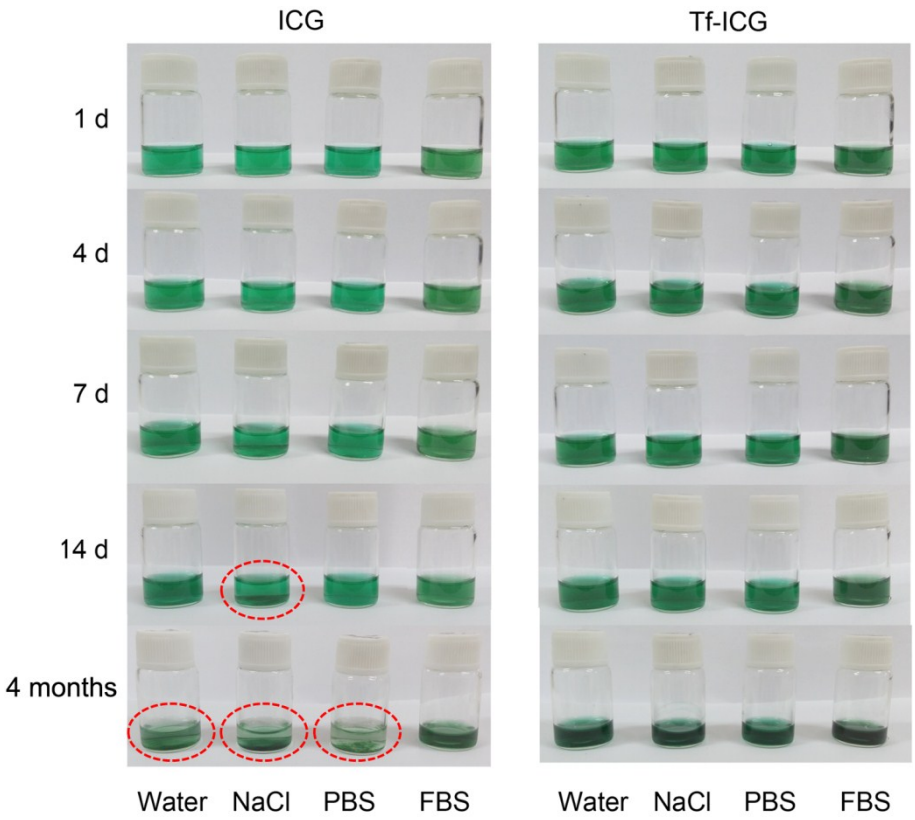

Fig. S1 Long-term colloidal stability of pure ICG (0.14 mg/mL) and Tf-ICG nanoparticles (1 mg/mL) dispersed in water, NaCl (w/w, 0.9%), PBS (pH 7.4, 10 mM), fetal calf serum (FBS), respectively. The concentration of ICG in Tf-ICG solution is equivalent to that of pure ICG, and the precipitations of ICG in water, NaCl solution and PBS were indicated by a red dashed cycle.

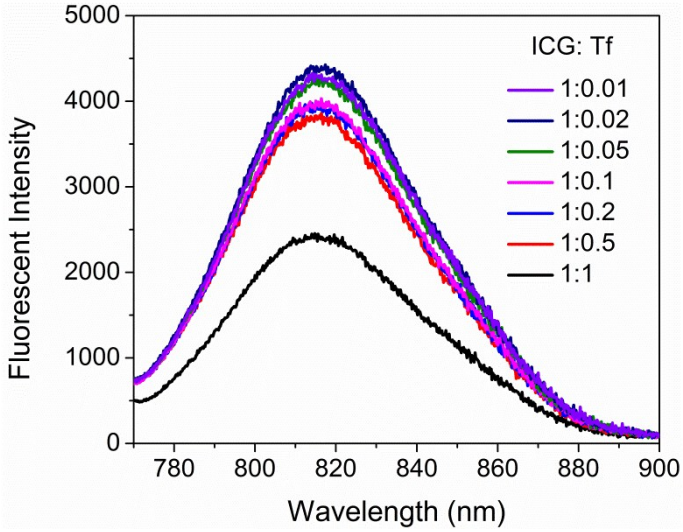

Fig. S2 The optimization of the molar ratio of ICG (4 μM) to Tf for the preparation of Tf-ICG nanoparticles based on the fluorescent spectra of ICG in the absence and presence of different concentrations of Tf.

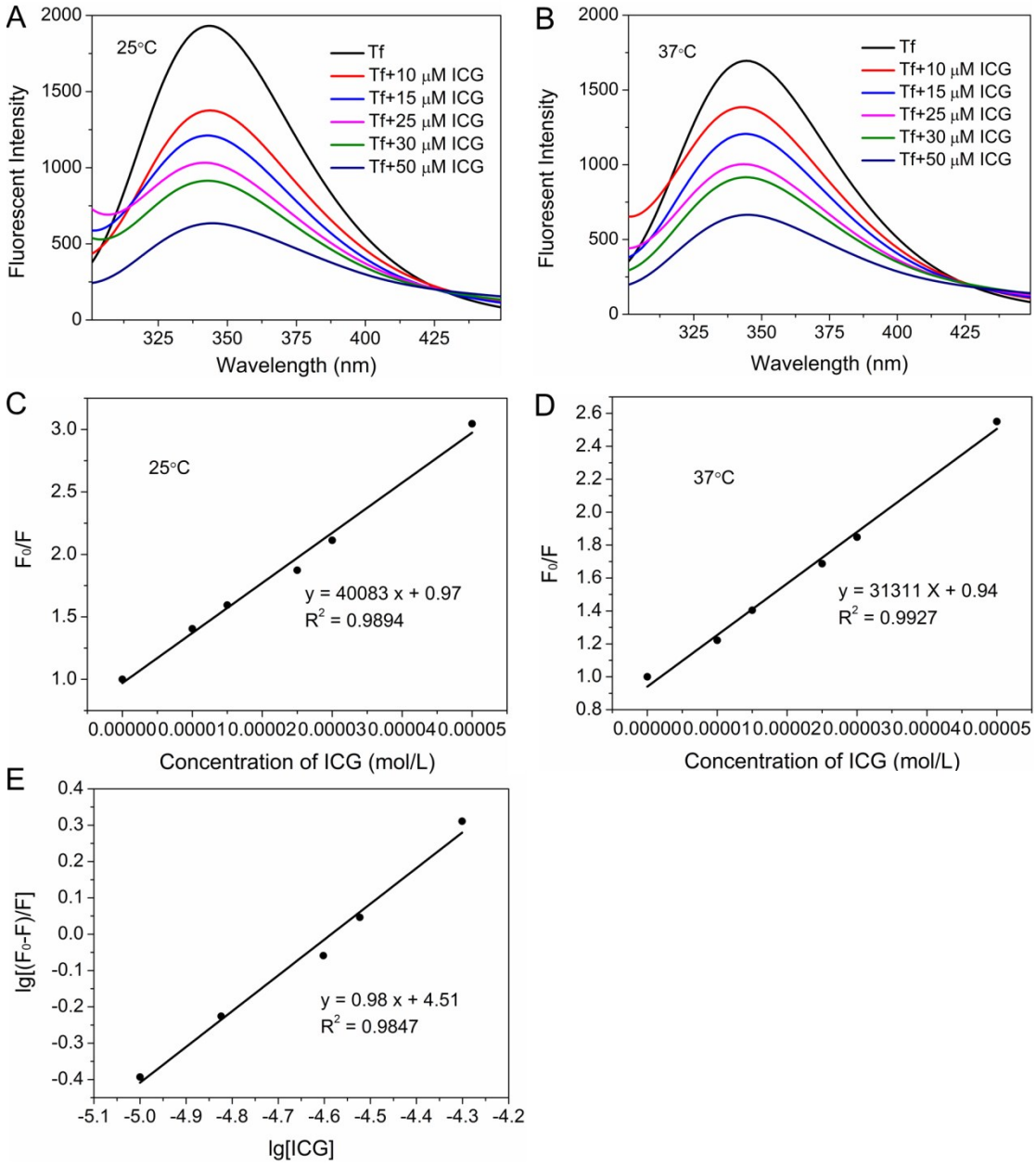

Fig. S3 The study of dynamic process of fluorescence quenching using the Stern-Volmer equation and the determination of the binding constant of Tf and ICG.[1,2] (A) Fluorescent spectra of Tf in the absence and presence of different concentrations of ICG at 25°C; (B) Fluorescent spectra of Tf in the absence and presence of different concentrations of ICG at 37°C; (C) Plot of F_0/F versus [ICG] for the transferrin-ICG system at 25°C; (D) Plot of F_0/F versus [ICG] for the transferrin-ICG system at 37°C; (E) Plot of lg[$(F_0$-F)/F] versus lg[ICG] for the transferrin-ICG system at 25°C.

Tf has several intrinsic fluorophores and could emit fluorescence with excitation at 265 nm. The fluorescence of Tf decreased regularly when a fixed concentration of Tf was titrated with different concentration of ICG in PBS buffer (10 mM, pH 7.4) at 25 or 37°C (Fig. S3A and B). The fluorescence quenching was analyzed by the Stern-Volmer equation:

$$\frac{F_0}{F} = 1 + K_{sv}[ICG]$$

F_0 and F are the fluorescence intensities of Tf in absence and presence of the quencher ICG, respectively. [ICG] is the concentration of ICG, and K_{sv} is the Stern-Volmer quenching constant. Based on the regression curves, the Stern-Volmer quenching constants were calculated to be 4.0×10^4 M^{-1} and 3.1×10^4 M^{-1} at 25°C and 37°C, respectively (Fig. S3C and D). The quenching constant K_{sv} decreased as the temperature increased, which indicated that a static quench process was operative by the formation of a Tf-ICG complex. The binding constant of Tf and ICG was determined by the following equation:

$$lg\frac{F_0 - F}{F} = lgK_a + nlg[ICG]$$

F_0 and F are the fluorescence intensities of Tf in absence and presence of the quencher ICG, respectively. K_a and n are the apparent binding constant and the number of binding site, respectively. Based on the double logarithm curves for Tf and ICG, the binding constant (K_a) was determined to be 3.2×10^4 M^{-1} at 25°C (Fig. S3E). The binding constant was big enough to ensure the formation of stable Tf-ICG self-assembly.

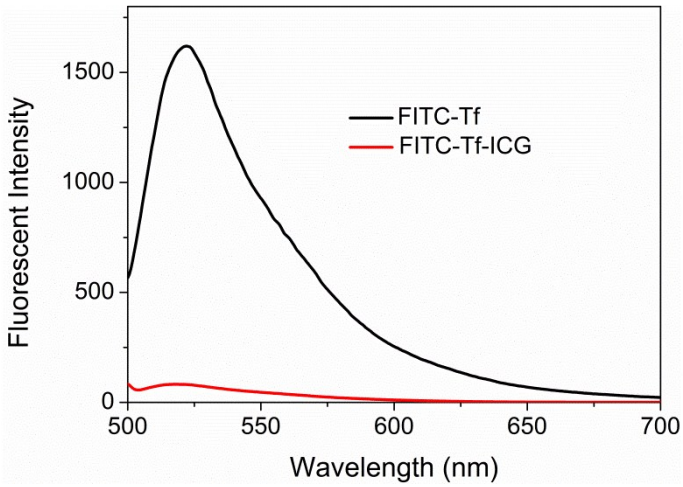

Fig. S4 Fluorescent spectra of FITC-labelled Tf and FITC-labelled Tf-ICG (0.15 mg/mL).

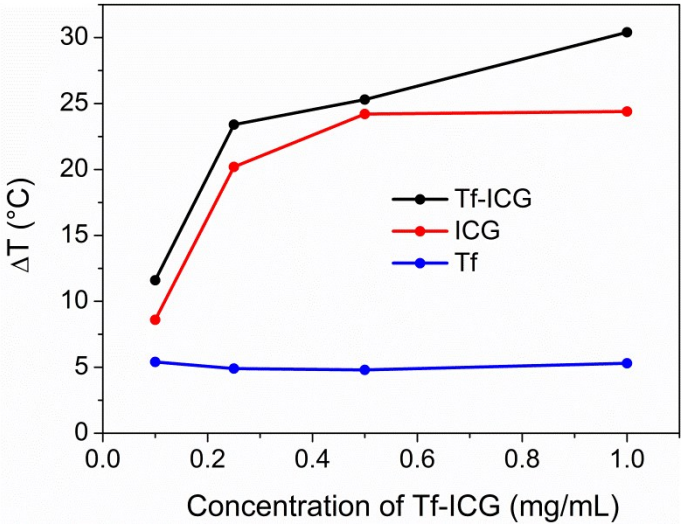

Fig. S5 The temperature change of Tf, ICG and Tf-ICG solution with different concentrations. The concentrations of Tf-ICG were ranged from 0.1 to 1 mg/mL, and the concentration of free ICG or Tf was equivalent to that in Tf-ICG nanoparticles, respectively.

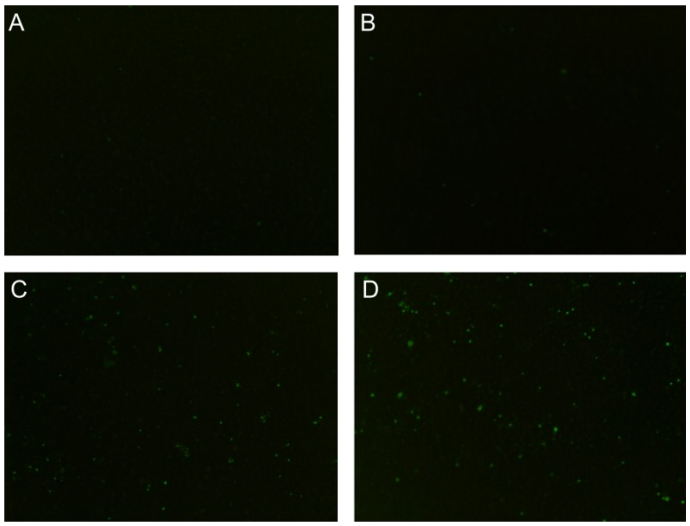

Fig. S6 The cellular fluorescent images of 3T3 and Hela cells with treatment of FITC-labelled Tf for the evaluation of Tf-receptor expressing levels. (A) 3T3 cells, 0.075 mg/mL FITC-labelled Tf, incubated for 24 h; (B) 3T3 cells, 0.15 mg/mL FITC-labelled Tf, incubated for 24 h; (C) Hela cells, 0.075 mg/mL FITC-labelled Tf, incubated for 24 h; (D) Hela cells, 0.15 mg/mL FITC-labelled Tf, incubated for 24 h.

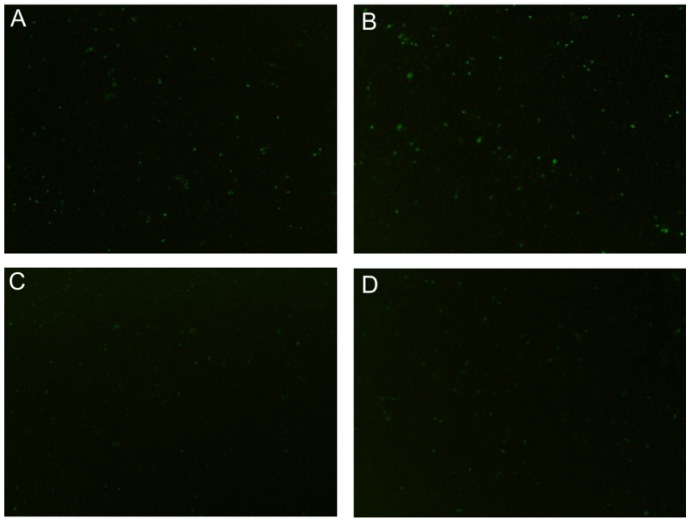

Fig. S7 The cellular fluorescent images of Hela cells with different treatments for the evaluation of receptor binding ability of Tf before and after loading of ICG. (A) 0.075 mg/mL FITC-labelled Tf, incubated for 24 h; (B) 0.15 mg/mL FITC-labelled Tf, incubated for 24 h; (C) FITC-labelled Tf-ICG (FITC-labelled Tf, 0.075 mg/mL), incubated for 24 h; (D) FITC-labelled Tf-ICG (FITC-labelled Tf, 0.15 mg/mL), incubated for 24 h.

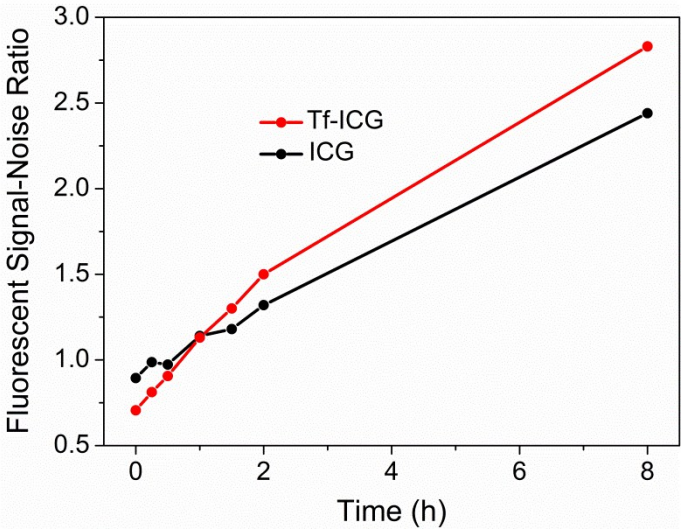

Fig. S8 Fluorescent signal-noise ratio of tumor regions of mice treated with Tf-ICG nanoparticles (200 μL, 7 mg/mL) or pure ICG (200 μL, 1 mg/mL) at different time points.

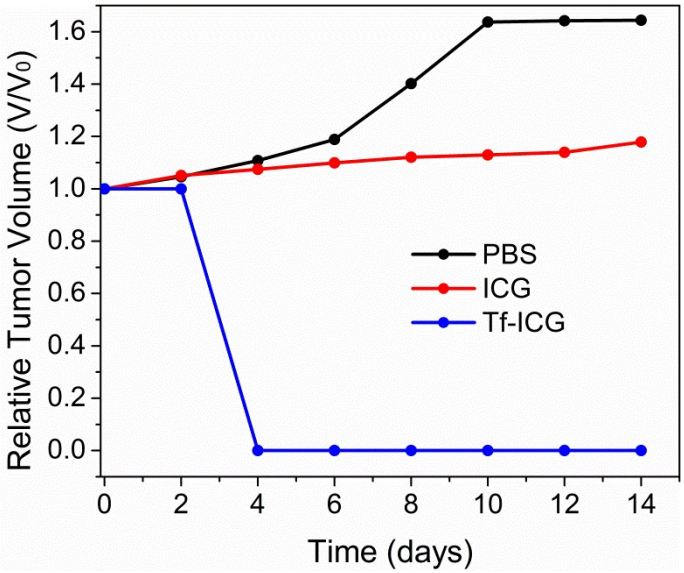

Fig. S9 Tumor growth curves of mice (n=5 in one group) treated with PBS, ICG (200 μL, 1 mg/mL) or Tf-ICG nanoparticles (200 μL, 7 mg/mL) and laser irradiation.

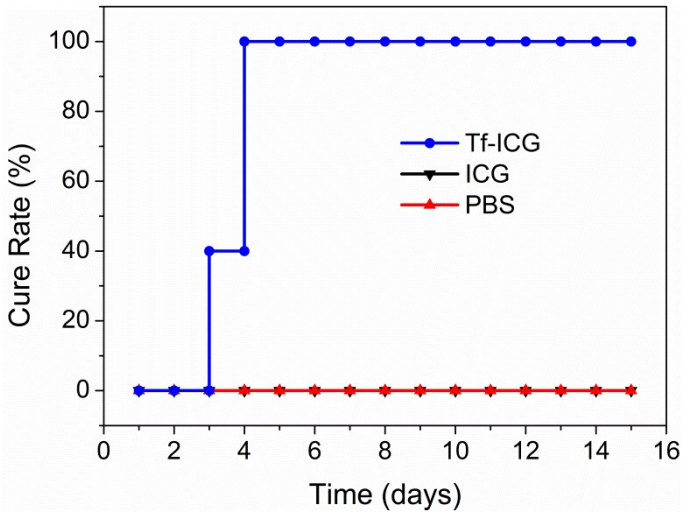

Fig. S10 The cure rate of mice treated with Tf-ICG nanoparticles, ICG or PBS and laser irradiation (5 mice in one group).

References

1 X.-f. Zhang, L. Lan, L. Chen, H.-b. Chen, Q.-f. Yang, Q. Li, Q.-l. Li, X.-r. Sun and Y.-l. Tang, *J. Phys. Org. Chem.* 2016, **29**, 127.

2 X.-f. Zhang, L. Chen, Q.-f. Yang, Q. Li, X.-r. Sun, H.-b. Chen, G. Yang and Y.-l. Tang, *Colloid Surface. A* 2015, **469**, 187.